CHEMISTRY
A EUROPEAN JOURNAL

DOI: 10.1002/chem.200600161

Reactivity of Lanthanocene Amide Complexes toward Ketenes: Unprecedented Organolanthanide-Induced Conjugate Electrophilic Addition of Ketenes to Arenes

Ruiting Liu,[a] Chunmei Zhang,[a] Zhenyu Zhu,[a] Jun Luo,[a] Xigeng Zhou,*[a, b] and Linhong Weng[a]

Abstract: This paper presents some unusual types of reactions of lanthanocene amide complexes with ketenes, and demonstrates that these reactions are dependent on the nature of amide ligands and ketenes as well as the stoichiometric ratio under the conditions involved. The reaction of $[\{Cp_2LnNiPr_2\}_2]$ with four equivalents of Ph_2CCO in toluene affords the unexpected enolization dearomatization products $[Cp_2Ln(OC\{2,5\text{-}C_6H_5(=CPh\text{-}CONiPr_2\text{-}4)\}=CPh_2)]$ (Ln = Yb (**1a**), Er (**1b**)) in good yields, representing an unprecedented conjugate electrophilic addition to a non-coordinated benzenoid nucleus. Treatment of $[\{Cp_2LnNiPr_2\}_2]$ with four equivalents of PhEtCCO under the same conditions gives the unexpected enolization dearomatization/rearomatization products $[\{Cp_2Ln(OC\{C_6H_4(p\text{-}CHEtCO\text{-}NiPr_2)\}=CEtPh)\}_2]$ (Ln = Yb (**2a**), Er (**2b**), Dy (**2c**)). However, reaction of $[\{Cp_2YbNiPr_2\}_2]$ with PhEtCCO in THF forms only the mono-insertion product $[Cp_2Yb\{OC(NiPr_2)=CEtPh\}](THF)$ (**3**). Hydrolysis of **2** afforded aryl ketone $PhEtCHCOC_6H_4(p\text{-}CHEtCONiPr_2)$ (**4**) and the overall formation of aryl ketone **4** provides an alternative route to the acylation of aromatic compounds. Moreover, reaction of $[\{Cp_2LnNHPh\}_2]$ with excess of PhEtCCO or Ph_2CCO in toluene affords only the products from a formal insertion of the C=C bond of the ketene into the N–H bond, $[(Cp_2Ln\{OC(CHEtPh)NPh\})_2]$ (Ln = Yb (**5a**), Y (**5b**)) or $[(Cp_2Er\{OC(CHPh_2)NPh\})_2]$ (**6**), respectively, indicating that an isomerization involving a 1,3-hydrogen shift occurs more easily than the conjugate electrophilic addition reaction, along with the initial amide attack on the ketene carbonyl carbon. $[\{Cp_2ErNHEt\}_2]$ reacts with an excess of PhEtCCO to give $[(Cp_2Er\{PhEtCHCON(Et)COCEtPh\})_2]$ (**7**), revealing another unique pattern of double-insertion of ketenes into the metal–ligand bond without bond formation between two ketene molecules. All complexes were characterized by elemental analysis and by their spectroscopic properties. The structures of complexes **1b**, **2a**, **2b**, **5a**, **5b**, **6**, and **7** were also determined through X-ray single-crystal diffraction analysis.

Keywords: acylation · conjugate addition · dearomatization · insertion · ketene · organolanthanide complexes

Introduction

The insertion of unsaturated substrates into organolanthanide complexes is regarded as one of the most fundamental organometallic reactions and has attracted great interest as a basis for the lanthanide-promoted functionalization and polymerization reactions.[1–6] Among these, the insertions of small unsaturated organic molecules into Ln–N bonds have received particular attention because of the potential to generate a carbon–nitrogen bond. Such stoichiometric insertions have resulted in a wide variety of new organolanthanides.[1,2b,5b,c,18] Additionally, catalytic transformation of unsaturated amines through the Ln–N bond insertion mechanism has yielded organic products that would only be accessible, often less selectively, by lengthy alternative synthetic routes.[7] Thus, the development of new insertions into the Ln–N bond is very desirable in organic synthesis and organolanthanide chemistry.

[a] R. Liu, C. Zhang, Z. Zhu, Dr. J. Luo, Prof. X. Zhou, L. Weng
Department of Chemistry and Shanghai Key Laboratory of Molecular Catalysis and Innovative Materials
Fudan University, Shanghai 200433 (P.R. China)
Fax: (+86) 21-6564-1740
E-mail: xgzhou@fudan.edu.cn

[b] Prof. X. Zhou
State Key Laboratory of Organometallic Chemistry Shanghai 200032 (P.R. China)

As the isoelectronic analogues of CO_2, ketenes have been observed to react with many transition-metal complexes to give the extensive products arising from simple addition of the ketene to the metal, insertion into the metal–ligand bond, reaction at coordinated ligands, transformation of the ketene into new ligands, and metal-induced conversion of the ketene into other organics.[8–10] Surprisingly, however, the organolanthanide chemistry of ketenes has remained almost unexplored to date,[11] even though this should be a fertile area since the increased Lewis acidity of the lanthanides could lead to new and interesting patterns of reactivity compared to their transition-metal counterparts.[12] Furthermore, to our knowledge, no previous examples of the double-insertion of ketenes into the metal–ligand bond are known. Recently, we reported the first insertion of ketenes into the metal–sulfur bond.[11] Given the remarkable reaction chemistry of organolanthanide amide complexes with other heteroallenes such as CO_2,[1c,2b] CS_2,[3] PhNCO,[4b,f] PhNCS,[3] and RNCNR,[5a–c] we decided to extend our studies to the insertion reactions of ketenes and in particular to the mechanism governing the stoichiometric mono- and bis-insertion reaction on metallocene amide derivatives of rare-earth metals.

On the other hand, the development of new methods for the efficient and selective preparation of polysubstituted alicyclic molecules is of great interest in organic synthesis because of the frequent existence of such structures in biologically active compounds and their role as valuable synthetic intermediates.[13–15] Among these newly developed methods, metal-catalyzed dearomatization has proven to be an attractive route to the preparation of such species.[13] Of particular importance is the partial dearomatization that allows the reactivity of the remaining unsaturation to be exploited.[15] In addition, the transformation of arenes, an abundant and inexpensive class of natural compounds, into more useful organic materials is desirable from the economic and environmental viewpoint.[16] Despite significant advances in the addition of substituents to the coordinated-benzenoid nucleus,[13] attempts to integrate any functionality directly on the non-coordinated nuclei of organometallic complexes has proved very difficult. To our knowledge, only a few steric bulky O-coordinated aryl aldehyde and ketone complexes, as well as arenes bearing a Fischer carbene appendage have ever been found to undergo the selective dearomatization through conjugate nucleophilic addition of carboanions, but their intermediate complexes have not been isolated and structurally characterized,[17] thus raising the intriguing question of whether the analogous conjugate electrophilic addition processes might also be feasible in dearomatization chemistry. Herein we describe the reactions of ketenes with a variety of lanthanocene amides, showing that the nature of the amide ligands strongly affects the chemo- and regioselectivity of these reactions and that the lanthanocene moiety can induce an unprecedented conjugate electrophilic addition of ketenes to the phenyl substituent of enolate ligands and the subsequent dearomatization, providing new routes to dearomatization and acylation of aromatic compounds. Furthermore, we observed that the use of primary amide ligands that contain a N–H bond, led not only to the isomerization of the newly formed amino-substituted enolate ligand to the amido ligand through a 1,3-hydrogen shift, but to the occurrence of another unusual double-insertion of ketenes into the metal–ligand bond.

Results and Discussion

Reactivity of [{Cp$_2$LnN*i*Pr$_2$}$_2$] towards diphenylketene: As part of our studies of the reactivity of organolanthanide amides towards unsaturated organic molecules,[4b,5c,18] we examined first the reaction of [{Cp$_2$LnN*i*Pr$_2$}$_2$] with Ph_2CCO. Addition of four equivalents of Ph_2CCO to a solution of [{Cp$_2$LnN*i*Pr$_2$}$_2$] in toluene gave the unexpected enolization–dearomatization products **1** in good yields. A possible reaction pathway for the formation of **1** is proposed in Scheme 1. In the initiation step, addition of the Ln–N*i*Pr$_2$ bond to the carbonyl group of Ph_2CCO would yield an amino-substituted enolate intermediate (**I**). As part of the negative charge is transferred from the oxygen to the aromatic ring through expanded conjugated systems, the pendent phenyl ring of the newly formed enolate ligand exhibits "electrophilic-like" reactivity,[19] leading to the subsequent attack of the phenyl-ring carbon atom to the incoming ketene molecule to form the conjugate electrophilic addition product **1**. However, attempts to isolate the single-insertion

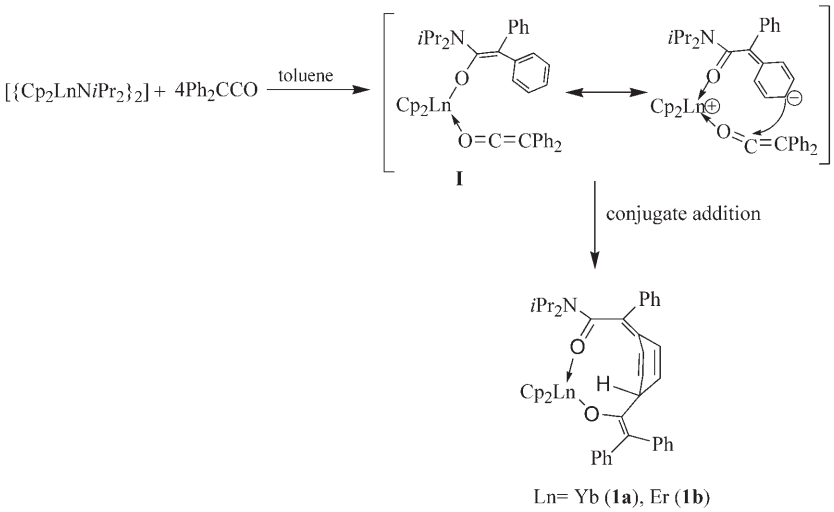

Scheme 1. Possible reaction pathway for formation of complex **1**.

intermediate were unsuccessful, indicating that the formation of **1** is competing with with the insertion of Ph_2CCO into the Ln–N bond of $[\{Cp_2LnNiPr_2\}_2]$ in toluene.

Relative to directly coordinated aryl rings, the selective transformation of a free aryl group to a cyclohexadienyl group is a much greater challenge.[20,21] The known examples of addition to the uncoordinated benzene nucleus of organometallic complexes are very rare and limited to nucleophilic addition of carbanions, where only both 1,4- and 1,6-addition modes are observed.[17] Accordingly, the substitution of the C–H group of the pendent aryl group is more common in comparison with the addition to the C=C unsaturated bond of the pendent aryl groups.[22] On the other hand, although the reaction chemistry of lanthanide complexes has been investigated extensively, only a few examples of dearomatization through a low-valent lanthanide reduction mechanism, are known and all of them are hydrogenation reactions.[19c,d,23] Furthermore, no example of dearomatization of aromatic ketenes has been reported previously.[8] To our knowledge, the present reaction represents not only the first example of trivalent lanthanide-driven functionalized dearomatization but also a new type of well-characterized conjugate electrophilic addition to the non-coordinated benzenoid nucleus, thus allowing the valuable direct introduction of oxygen-containing functional groups onto the resulting alicyclic ring in the process of dearomatization that is impossible for other dearomatization methods.

Complexes **1a** and **1b** are soluble and stable in toluene and THF, and do not undergo rearomatization or isomerization under ambient conditions. The spectroscopic properties of **1a** and **1b** are very similar, indicating that they have the same structures. Only one of them, **1b**, was characterized crystallographically. In the mass spectra, all the compounds clearly display their molecular ions.

The structure of complex **1b**, which crystallizes from a solvent mixture of toluene and hexane in the tetragonal system, space group *P*4/*n*, is shown in Figure 1, and selected bond lengths and angles are given in Table 1. The X-ray structure of complex **1b** definitively proves that a second Ph_2CCO is attached at the *para* position of the phenyl ring of the first Ph_2CCO unit inserted into a Ln–N bond through a conjugate electrophilic addition reaction. Complex **1b** is a solvent-free mononuclear structure with the erbium atom bonded to two η^5-cyclopentadienyl rings and two chelating oxygen atoms. Bond angles around the C(25) atom are consistent with sp^3 hybridization. The cyclohexadiene part of complex **1b** features the expected long-long-short-long-long-short array of carbon–carbon bonds along the six-membered ring. As a result, the ring is severely distorted, adopting a "boat" type of conformation. The C(26), C(27), C(29), and C(30) atoms lie coplanar within experimental error. The C(25) and C(28) atoms are out of the plane by 0.26 and 0.19 Å, respectively. Bond lengths and angles within the vinyl-oxo ligand are as expected, with the C(11)–O(1) distance having "single-bond" character, and the C(38)–O(2) distance having double-bond character.[2b,24–26] The coordination environment around the erbium atom in **1b** is typical of trivalent $(C_5H_5)_2Er$-containing complexes, and the complex has no unusual lengths or angles in the Cp_2Er unit (Table 1). The Er(1)–O(1) distance of 2.126(6) Å is similar to that observed for Cp_2ErOR-type complexes,[27] whereas the Er(1)–O(2) distance of 2.297(6) Å is at the low end of the range typical for Cp_2ZEr-OR_2 donor bonds (Z = a monoanionic ligand).[28] The O-Er-O angle of 117.9(2)° is significantly larger than typical donor atom-metal-donor atom angles in compounds of this type due to the rigidity of the cyclohexadiene unit.[4e,19a]

Table 1. Selected bond lengths [Å] and angles [°] of complex **1b**.

Er(1)–O(1)	2.126(6)	Er(1)–O(2)	2.297(6)
C(11)–O(1)	1.314(10)	C(27)–C(28)	1.452(12)
C(11)–C(12)	1.374(12)	C(28)–C(31)	1.349(12)
C(11)–C(25)	1.555(13)	C(28)–C(29)	1.465(13)
C(12)–C(19)	1.469(14)	C(29)–C(30)	1.328(13)
C(12)–C(13)	1.496(13)	C(31)–C(32)	1.489(11)
C(25)–C(26)	1.472(12)	C(31)–C(38)	1.513(12)
C(25)–C(30)	1.483(14)	C(38)–O(2)	1.248(10)
C(26)–C(27)	1.344(12)	C(38)–N(1)	1.325(11)
O(1)-Er(1)-O(2)	117.9(2)	C(31)-C(28)-C(27)	120.2(8)
O(1)-C(11)-C(12	126.3(9)	C(31)-C(28)-C(29)	123.7(9)
O(1)-C(11)-C(25)	112.3(8)	C(27)-C(28)-C(29)	116.1(8)
C(12)-C(11)-C(25)	121.3(8)	C(30)-C(29)-C(28)	120.0(9)
C(11)-C(12)-C(19)	123.8(9)	C(29)-C(30)-C(25)	123.3(9)
C(11)-C(12)-C(13)	118.6(9)	C(28)-C(31)-C(32)	126.9(8)
C(19)-C(12)-C(13)	117.6(8)	C(28)-C(31)-C(38)	115.9(8)
C(26)-C(25)-C(30)	111.4(8)	C(32)-C(31)-C(38)	116.8(7)
C(26)-C(25)-C(11)	107.3(8)	O(2)-C(38)-N(1)	122.3(9)
C(27)-C(26)-C(25)	122.8(9)	O(2)-C(38)-C(31)	118.0(8)
C(26)-C(27)-C(28)	120.1(8)	N(1)-C(38)-C(31)	119.6(8)

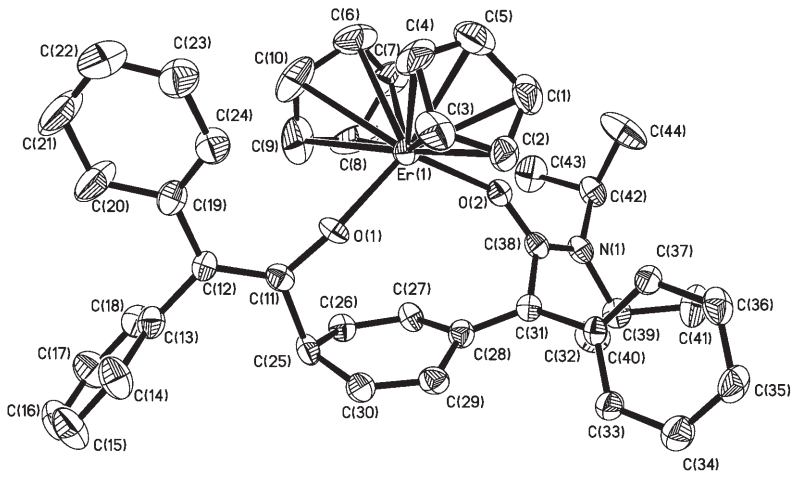

Figure 1. Molecular structure of complex **1b** (thermal ellipsoids at 30% probability).

Reactivity of [{$Cp_2LnNiPr_2$}$_2$] towards ethylphenylketene: Enolate groups are important ligands in organometallic chemistry because they are related to many metal-mediated transformations of aldehydes and ketones. However, little is known about the structures and the reactivities of rare-earth organometallic complexes containing this kind of ligand so far.[19,24,25] To obtain additional insight into the mechanism and scope of the lanthanide-induced transformation of aryl-substituted enolate ligands, we examined the behavior of [{$Cp_2LnNiPr_2$}$_2$] towards PhEtCCO. In contrast to the reaction of Ph_2CCO, treatment of [{$Cp_2LnNiPr_2$}$_2$] with four equivalents of PhEtCCO under the same conditions gave another unexpected coupling-insertion/isomerization products [{$Cp_2Ln(OC\{C_6H_4(p\text{-}CHEtCONiPr_2)\}{=}CEtPh)$}$_2$] (Ln = Yb (**2a**), Er (**2b**), Dy (**2c**)). The formation of **2** can be interpreted as the conjugate electrophilic addition of the incoming ketene molecule to the phenyl-substituted enolate ligand derived from PhEtCCO insertion into the Ln–N bond (as observed in the formation of **1**) followed by rearomatization, which involves a 1,5-hydrogen shift (Scheme 2).

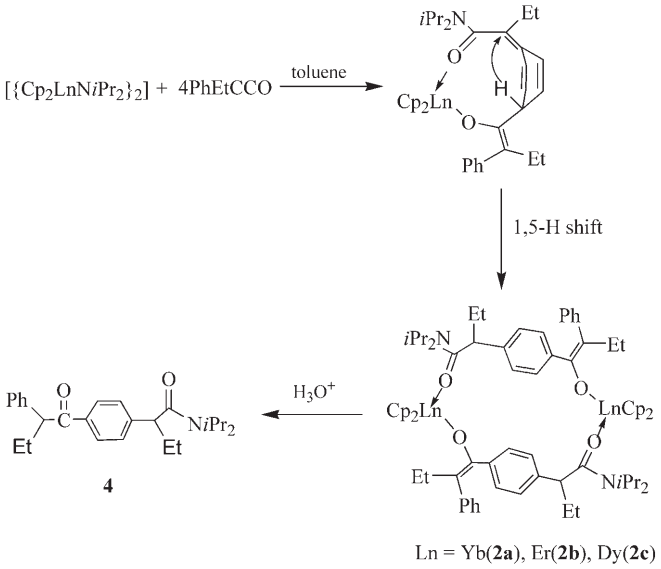

Scheme 2. Scheme showing the formation of complex **2.**

Interestingly, the nature of the ketenes regulates the hydrogen migration. In the case of Ph_2CCO, since the increasing steric congestion results in a large distance between the C(25) and C(31) atoms (e.g., 4.18 Å found in **1b**, Figure 1), the corresponding hydrogen shift is prevented. Furthermore, the π–π conjugation of the additional phenyl moiety also incurs a favorable stabilization on **1**. These results demonstrate that the steric and electronic factors greatly influence rearomatization of the conjugated addition intermediates.

Multiple insertion of unsaturated substrates into the metal–ligand bond is the key step in the propagation of the chain. Consequently, a good understanding of factors that promote or deter multiple insertion would permit the control of this reaction and enable design of new catalysts for polymerization and transformation of substrates. Although insertions of polar heterocumulenes into the M–N, M–C, and M–O bonds have been studied with a variety of metals, only a limited number of multiple insertions are known.[29] Well-characterized reactions involving multiple insertions are mainly those of alkynes,[30] nitriles,[31] isocyanides,[4e] and carbon monoxide.[32,4e] To the best of our knowledge, the formation of **1** and **2** represents the first example of the ketene coupling insertion into the metal–ligand bond.[8–11] In addition, this type of aryl coupling–insertion is highly unusual and has not been authenticated previously for other aryl-substituted unsaturated substrates. In previously reported coupling–insertion reactions, cumulenes are always incorporated through X=C=Y centers. Therefore, the results demonstrate the ketenes can be expected to undergo distinctive reactivity beyond that possible with other cumulenes.

It is noteworthy that the formation of **2** is also competing with the insertion of PhEtCCO into the Ln–N bond of [{$Cp_2LnNiPr_2$}$_2$] in toluene. For example, complex **2a** was also obtained and isolated in low yield when [{$Cp_2YbNiPr_2$}$_2$] was treated with two equivalents of PhEtCCO in toluene. However, treatment of [{$Cp_2YbNiPr_2$}$_2$] with two equivalents of ethylphenylketene allowed us to isolate the mono-insertion product [$Cp_2Yb\{OC(NiPr_2){=}CEtPh\}$](THF) (**3**) in a good yield when the reaction was carried out in THF [Eq. (1)].

$$[\{Cp_2YbNiPr_2\}_2] + 2\,PhEtCCO \xrightarrow{THF} 2\,[Cp_2Yb\{OC(NiPr_2){=}CEtPh\}](THF) \quad (1)$$

The ease with which the double-insertion of ketene into the Ln–N bond occurs in toluene as opposed to the mono-insertion observed in THF emphasizes the crucial role that the metal—ketene coordination plays before the attack of the phenyl on the carbonyl of ketene can occur. Such a pre-coordination seems to have a double function by providing a close geometrical proximity for the attack of the pendent phenyl group on the carbonyl and increasing the polarization of the ketene. Since the coordination of the second ketene moiety to the metal center in THF, a prerequisite for further reactivity, is likely to be inhibited by the coordinated THF, selective formation of the mono-insertion product can occur.

Complexes **2** and **3** have been characterized by elemental analysis, IR and ^{1}H NMR spectroscopy, and mass spectrometry, which gave results that were in good agreement with the proposed structures. The structures of compounds **2a** and **2b** were determined by X-ray diffraction analysis. A selection of interatomic distances is given in Table 2. For comparison purposes, a common atomic numbering scheme has been used. Attempts were also made to obtain structural information in the solid state for the complex **3**, but the poor quality of the obtained crystals prevented any X-ray analysis.

As shown in Figure 2, complexes **2a** and **2b** are isomorphous, in which a newly formed aryl-substituted enolate

Table 2. Selected bond lengths [Å] and angles [°] for complexes **2a** and **2b**.

	Ln = Yb (**2a**)	Ln = Er (**2b**)
Ln–O(2A)	2.070(7)	2.120(10)
Ln–O(1)	2.227(7)	2.248(7)
O(1)–C(11)	1.260(11)	1.282(12)
O(2)–C(27)	1.320(12)	1.333(16)
C(11)–C(12)	1.524(13)	1.502(16)
C(12)–C(13)	1.504(12)	1.535(15)
C(16)–C(27)	1.510(13)	1.452(16)
C(27)–C(28)	1.320(4)	1.315(19)
Ln–C_{av}(Cp)	2.650(12)	2.655(13)
Ln–Ln	8.773	8.845
O(2A)-Ln-O(1)	93.6(2)	92.9(3)
C(11)-O(1)-Ln	167.6(6)	165.1(6)
C(27)-O(2)-Ln	160.8(6)	161.7(7)
O(1)-C(11)-C(12)	116.2(9)	117.8(9)
C(11)-C(12)-C(13)	110.8(8)	111.6(9)
C(28)-C(27)-O(2)	124.6(9)	120.7(13)
C(28)-C(27)-C(16)	121.4(10)	127.1(16)
O(2)-C(27)-C(16)	114.0(9)	112.2(11)
(17)-C(16)-C(27)	122.7(10)	122.2(12)

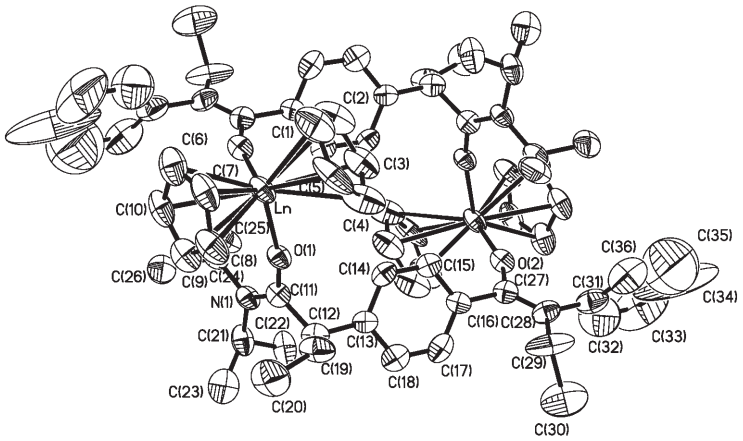

Figure 2. Molecular structure of complex **2a** (Ln = Yb) and complex **2b** (Ln = Er) (thermal ellipsoids at 30% probability).

ligand is clearly established and acts as a bidentate anion to connect the two Cp_2Ln units through both oxygen atoms, forming a centrosymmetric metallacyclic structure. Each metal is coordinated by two η^5-C_5H_5 groups, one enolate oxygen atom and one donor oxygen atom from another OC(C_6H_4(*p*-CHEtCON*i*Pr_2))=CEtPh ligand in a distorted tetrahedral geometry. The Yb–O(2A) distance of 2.070(7) Å in **2a** is considerably shorter than the Yb–O(1) bond length of 2.227(7) Å, indicating that the negative charge transfer took place from one oxygen to another through the aromatic ring along with the incorporation of the second ketene. Namely, the O(2) atom is part of a formally anionic enolate ligand, while the O(1) oxygen is part of a neutral carbonyl group. The O(2)–C(27) bond (1.320(12) Å) is longer than the O(1)–C(11) bond (1.260(11) Å), which is also consistent with the C(sp^2)–O single-bond character of the enolate versus the C=O double bond of the coordinated carbonyl group.[2b,24–26] The phenyl group attached to the C(27) atom has a single bond between the C(27) and C(16) atoms (1.510(13) Å), and there is a localized C=C double bond between the C(27) and C(28) atoms (1.320(4) Å). The middle C(13)–C(18) ring retains its aromaticity and is tilted at an angle of 55° to the C(31)–C(36) phenyl ring. The O-Yb-O angle of 93.6(2)° is larger than typical O-Ln-O angles (67–78°) in other dinuclear compounds.[11,33] It is noteworthy that the Yb–Yb distance of 8.773 Å is the longest observed in dinuclear organolanthanide structures. The rather long metal–metal distance may be attributed to both the rigidity of the aryl ring and the large steric crowding.

All bond parameters for complex **2b** are in normal ranges (Table 2), indicating that a second equivalent of ethylphenylketene was incorporated into the first insertion product through a tandem conjugate electrophilic addition/isomerization process, along with charge transfer from one oxygen atom to another through the aromatic ring. The bond lengths involving the metal in complex **2b** are similar to the corresponding values in complex **2a**, if the difference in metal radii is considered.[2b] The newly formed OC{C_6H_4(*p*-CHEtCON*i*Pr_2)}=CEtPh ligand bears an enolate bond at the one end, and the penultimate carbonyl group is coordinated to another Er atom. The enolate C=C and C–O distances (1.315(19) and 1.282(12) Å, respectively) in complex **2b** are comparable to the corresponding values found in *cis*-[{(C_5Me_5)$_2$(Ph_3PO)Sm}$_2$(μ-OCH=CHO)],[24] [{($CH_3C_5H_4$)$_2$Y(μ-OCH=CH_2)}$_2$],[25] and [Cp_2Ti(OCH=CH_2)$_2$].[26] However, the enolate O–C=C bond angle of 120.7(13)° is significantly smaller than those found in the metal enolates mentioned above.[24–26]

Hydrolysis of compound **2** afforded the aryl ketone PhEtCHCOC_6H_4(*p*-CHEtCON*i*Pr_2) (**4**) (Scheme 2). The overall formation of compound **4** is the synthetic equivalent of a directed *para* acylation of an aromatic ring bearing an inactive group, a process not readily achieved by using previously reported methods.[34] Thus, this new approach would complement the powerful techniques already available for the introduction of acyl substituents onto aromatic rings.

Reaction of [{Cp_2LnNHPh}$_2$] with ethylphenylketene and diphenylketene: With the aim of establishing whether the nature of amide ligands would govern the reaction like ketenes, the insertion of a ketene into lanthanocene primary amide complexes was also studied. In marked contrast to [{Cp_2LnN*i*Pr_2}$_2$], however, treatment of [{Cp_2LnNHPh}$_2$] with an excess of PhEtCCO in toluene, even with a higher reaction temperature and a longer reaction time, provided

only complexes **5** (Scheme 3), suggesting that an isomerization involving a 1,3-hydrogen shift occurs more easily than the conjugate electrophilic addition reaction, along with the initial amide attack to the ketene carbonyl carbon. In addition, we found that increasing the relative amounts of Ph_2CCO also had no influence on the product in the reaction of $[\{Cp_2ErNHPh\}_2]$ with Ph_2CCO, a single insertion only being observed. Evidently, the different chemoselectivity encountered for the formation of compounds **5** and **6** with respect to that of **1** and **2** can be rationalized assuming proton transfer from the nitrogen of the amino-substituted enolate intermediate to the less-acidic carbon atom, leading to the absence of the conjugate effect between the aromatic ring and the coordinated amido anion that is resistant to the charge transfer to the aromatic ring. These results again demonstrate that substantial negative charge transfer from the oxygen to the aromatic ring is required in the above conjugate electrophilic addition processes.

A similar formal insertion of the C=C bond of the ketene into the N–H bond was reported for nickel(II) and rhenium(I) primary amide complexes.[9] In addition, the transition-metal *N*-metallaimine reacted with ketenes to afford metal N-substituted β-lactams.[10] A major difference with respect to complexes **5** and **6** is that the transition-metal products feature an N-bonded monodentate amido ligand. The formation of a chelating amido linkage in our lanthanide complexes is enforced by the unsaturated nature and the oxophilicity of the lanthanocene fragment. Therefore, it is possible to envisage that the intermediate in this reaction is an amino-substituted enolate formed directly through the four-membered-ring transition state rather than the zwitterionic species as proposed in the reaction of ketenes with transition-metal amide complexes.[9,35]

The bonding mode of the resulting amido ligand was verified by the X-ray analysis of complexes **5a** and **5b** (Figure 3). A C=N stretching frequency in the IR spectrum at approximately 1580 cm^{-1} is in agreement with the bidentate η^3-bonding mode of the amido ligand,[36] and is significantly lower than those of monodentate amido ligands.[9] Also, the N–H stretching band that appeared at about 3300 cm^{-1} in the IR spectrum of $[\{Cp_2LnNHPh\}_2]$ was no longer present.[37]

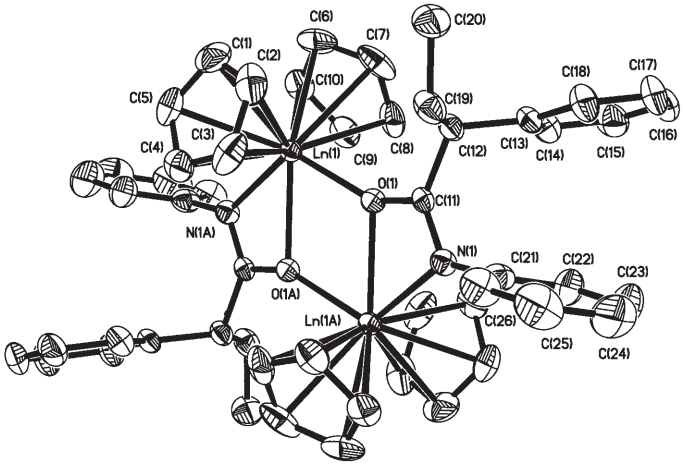

Figure 3. Molecular structure of complexes **5a** (Ln = Yb) and **5b** (Ln = Y) (thermal ellipsoids at 30% probability).

For complex **5a**, the X-ray analysis shows that the OCN fragment of the amido ligand acts as both a bridging and side-on chelating group, in which the negative charge is delocalized over the OCN unit. The corresponding isomerization involving a 1,3-hydrogen shift is unambiguously identified by the relative bond lengths and angles. The amido unit bridges the two Yb atoms through the oxygen atom, while the nitrogen atom in the newly formed ligand chelates to just one metal to give a formal coordination number of nine to each Yb atom. The eight atoms Yb(1), N(1A), C(11A), O(1A), Yb(1A), N(1), C(11), and O(1) form an interlinked tricyclic structure through the two bridging Yb(1)–O(1A), and Yb(1A)–O(1) bonds. Complex **5a** has normal metrical parameters in the metallocene part of the molecule (Table 3). The O-Yb-O angle of 68.0(1)° is within the 67.6(9)–78.0(4)° range of the corresponding values observed in other dinuclear oxygen-bridging complexes.[11,33] The Yb(1)–C(11A) distance of 2.846(4) Å is longer than the average Yb–C(η^5-Cp) distance, indicating a weak interaction between Yb(1) and C(11). Characteristically, complex **5a** has two distinctive metal–oxygen distances. The Yb(1)–O(1) distance of 2.283(3) Å is between those expected for an Yb^{3+}–O single bond and an $Yb^{3+}\leftarrow$O donor bond, while the Yb(1A)–O(1) distance of 2.410(3) Å falls in the 2.30(1)–2.50(1) range of the $Yb^{3+}\leftarrow OR_2$ donating bond lengths for neutral oxygen donor ligands.[38] However, two bridging Ln–O distances are generally similar in other dimeric oxygen-bridging organolanthanide com-

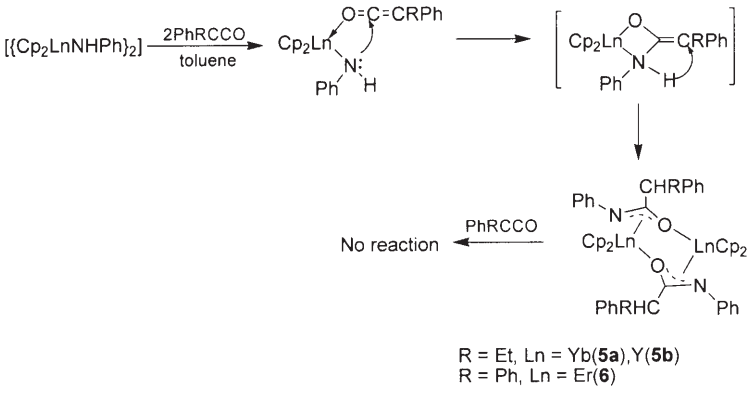

Scheme 3. Reaction of $[\{Cp_2LnNHPh\}_2]$ with ketene to yield complexes **5** and **6.**

Table 3. Selected bond lengths [Å] and angles [°] of complexes **5a** and **5b**.

	Ln = Yb (**5a**)	Ln = Y (**5b**)
Ln(1)–O(1)	2.283(3)	2.287(9)
Ln(1)–N(1A)	2.396(4)	2.416(10)
Ln(1)–O(1A)	2.410(3)	2.426(8)
Yb(1A)–C(11)	2.846(4)	2.852(6)
Ln(1)–C(2)	2.603(6)	2.601(15)
Ln(1)–C(3)	2.614(6)	2.605(16)
Ln(1)–C(7)	2.616(6)	2.609(14)
Ln(1)–C(4)	2.619(5)	2.628(13)
Ln(1)–C(1)	2.625(6)	2.629(15)
Ln(1)–C(8)	2.629(5)	2.633(15)
Ln(1)–C(6)	2.633(6)	2.637(14)
Ln(1)–C(10)	2.635(5)	2.641(14)
Ln(1)–C(9)	2.636(5)	2.643(14)
O(1)–C(11)	1.321(5)	1.299(15)
N(1)–C(11)	1.280(6)	1.264(15)
N(1)–C(21)	1.438(6)	1.407(17)
C(11)–C(12)	1.529(6)	1.518(14)
O(1)-Ln(1)-N(1A)	121.36(12)	121.0(3)
O(1)-Ln(1)-O(1A)	67.97(12)	68.4(3)
N(1A)-Ln(1)-O(1A)	54.05(12)	53.1(3)
C(11)-O(1)-Ln(1)	152.0(3)	152.5(8)
C(11)-O(1)-Ln(1A)	94.9(2)	95.1(7)
Ln(1)-O(1)-Ln(1A)	112.03(12)	111.6(3)
C(11)-N(1)-Ln(1A)	96.7(3)	96.6(9)
N(1)-C(11)-O(1)	114.2(4)	115.2(11)
N(1)-C(11)-C(12)	128.4(4)	127.3(13)
O(1)-C(11)-C(12)	117.4(4)	117.5(10)
N(1)-C(11)-Ln(1A)	56.7(2)	57.3(7)
O(1)-C(11)-Ln(1A)	57.5(2)	57.9(6)
C(12)-C(11)-Ln(1A)	174.0(3)	174.9(9)

plexes, such as $[\{Cp_2Ln(\mu\text{-}OR)\}_2]$[39] and $[\{(C_5H_4Me)Ln(\eta^2\text{-}PzMe_2)(\mu\text{-}\eta^1{:}\eta^2\text{-}OSiMe_2PzMe_2)\}_2]$.[40] This difference may be attributed to the steric effect caused by the side-on chelating coordination of the Yb^{3+} ion to the amido ligand.

The structural parameters of complex **5b** (Table 3) are very similar to those found in **5a.** The C(11)–C(12) distance of 1.518(14) Å is in the observed range for the C–C single bond distance. Both the O(1)–C(11) and the N(1)–C(11) distances of 1.299(15) and 1.264(15) Å lie between single- and double-bond lengths,[2b,41] suggesting electronic delocalization over the OCN unit. The Y–O and Y–N distances are comparable to the corresponding values in complex **5a**, respectively, when the difference in the metal ionic radii is considered. The Y–C(Cp) distances range from 2.601(15) to 2.643(14) Å, and the average value of 2.625(14) Å is similar to those found in other Cp_2Y-containing lanthanide complexes, such as $[\{(C_5H_5)_2Y(\mu\text{-}CH_3)\}_2]$, 2.66(2) Å[42a] and $[(C_5H_5)_2Y(\mu\text{-}CH_3)_2AlMe_2]$, 2.62(4) Å.[42b]

The structural features of compound **6** (Figure 4) are very similar to those of the products from insertion of isocyanate into the Ln–C bond of Cp_2LnR (R = *n*-butyl, α-naphthalenyl).[4c] The oxygen atom of the amido ligand is at a bridging position, and thus the OCN fragment of the amido ligand acts as both a bridging and side-on chelating group where the negative charge is delocalized over the OCN unit. This structure can be directly compared with those of complexes **5a** and **5b**. It is reasonable for compound **6** that the Er(1)–O(1) bond is longer than the Er(1A)–O(1) bond compared with the observations in complexes **5a** and **5b**. The Er(1)–N(1) distance of 2.435(5) Å is slightly shorter than that of the simple Er←:N donor bond,[43] and there is a weak interaction between the Er(1) and C(17) atoms. All bond parameters in the rest of the chelating ligand are in normal ranges (Table 4). The bond lengths involving the metal in complex **6** are similar to the corresponding values in complexes **5a** and **5b**, if the difference in metal radii is considered.

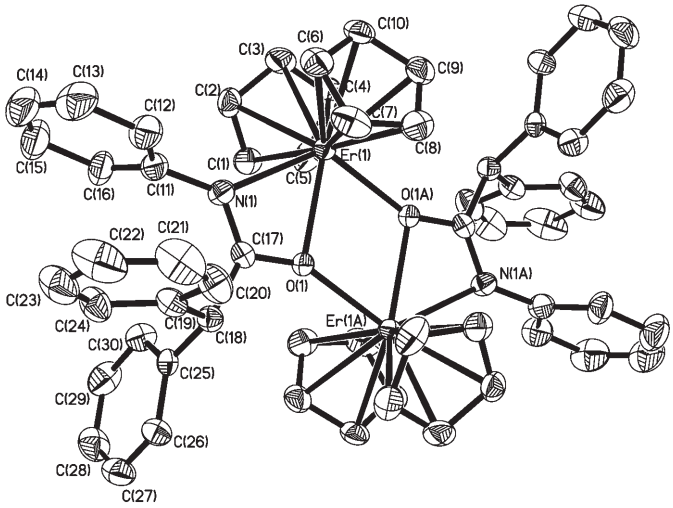

Figure 4. Molecular structure of complex **6** (thermal ellipsoids at 30% probability).

Table 4. Selected bond lengths [Å] and angles [°] of complex **6**.

Er(1)–O(1A)	2.303(4)	Er(1)–C(8)	2.645(7)
Er(1)–O(1)	2.390(4)	Er(1)–C(7)	2.646(7)
Er(1)–N(1)	2.435(5)	Er(1)–C(6)	2.648(6)
Er(1)–C(1)	2.626(6)	O(1)–C(17)	1.323(7)
Er(1)–C(9)	2.627(7)	O(1)–Er(1A)	2.303(4)
Er(1)–C(4)	2.633(7)	N(1)–C(17)	1.283(7)
Er(1)–C(5)	2.635(7)	N(1)–C(11)	1.438(8)
Er(1)–C(2)	2.637(7)	C(17)–C(18)	1.537(8)
Er(1)–C(10)	2.640(6)	Er(1)–C(17)	2.858(4)
O(1A)-Er(1)-O(1)	69.01(15)	C(11)-N(1)-Er(1)	138.4(4)
O(1A)-Er(1)-N(1)	122.86(15)	N(1)-C(17)-O(1)	114.0(5)
O(1)-Er(1)-N(1)	53.87(15)	N(1)-C(17)-C(18)	129.4(6)
C(17)-O(1)-Er(1A)	152.6(4)	C(17)-N(1)-Er(1)	95.4(4)
C(17)-O(1)-Er(1)	96.4(3)	N(1)-C(17)-Er(1)	58.0(3)
Er(1A)-O(1)-Er(1)	110.99(15)	O(1)-C(17)-Er(1)	56.2(3)
C(17)-N(1)-C(11)	126.1(5)	C(18)-C(17)-Er(1)	169.0(4)

Reaction of $[\{Cp_2ErNHEt\}_2]$ with ethylphenylketene: To further probe the factors that determine the alternative reaction pathways, we decided to extend our study on the ketene insertion of lanthanocene amides. Interestingly, by replacing NHPh with NHEt, the non-coupling double-insertion product **7** could be obtained as pink crystals from the 1:4 reaction between $[\{Cp_2ErNHEt\}_2]$ and PhEtCCO, which reveals another novel reactivity of organometallic complexes towards ketenes (Scheme 4). Although no intermediate (e.g., an amido complex) could be isolated in the reaction, a

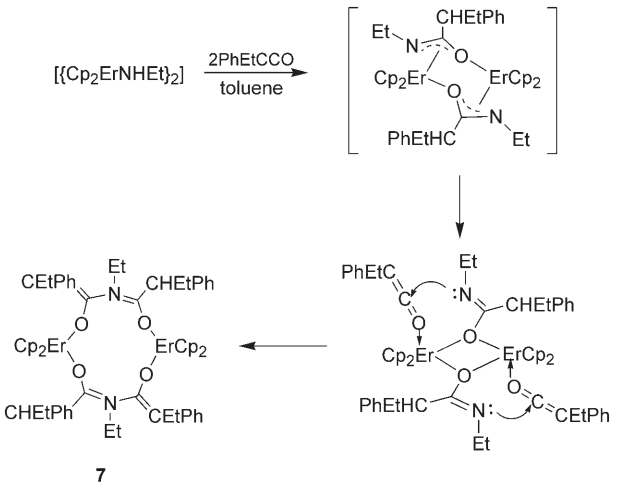

Scheme 4. Reaction pathway to produce compound **7.**

pathway similar to that proposed for the formation of complex **5** is very likely to account for the formation of complex **7**. Namely, the formation of complex **7** can be rationalized by a second ketene insertion into a non-isolable lanthanocene amido intermediate resulting from the first PhEtCCO insertion into a Ln–N bond of $[\{Cp_2LnNHEt\}_2]$ followed by a 1,3-hydrogen shift. The last step of Scheme 4 has also been proposed to explain the isocyanate coupling-insertion reaction into the Ln–C bond.[4e] An important characteristic of the present reaction is its unique pattern of double insertion without ketene molecules coupling to each other. In previously reported double insertions into the metal–ligand single bond, two substrate molecules are generally linked together, whereas the double insertions without bond formation between substrates are rare and are mainly limited to the cycloaddition of unsaturated substrates to the metal–ligand double bonds such as M=NR.[44] The reasons why $[\{Cp_2YbNHPh\}_2]$ does not react with a second ketene under the same conditions while $[\{Cp_2ErNHEt\}_2]$ does are as yet unclear, but may reflect the more steric demands of the phenyl group in comparison to the ethyl group.

The amino-substituted enolate complex intermediates react with a second equivalent of ketene to give the conjugated addition products involving the aryl ring, while the reaction of the amido complex with a second equivalent of ketene leads to the formation of the Ln–N addition product instead of the Ln–C one. This difference between the reactivities of $[\{Cp_2LnNiPr_2\}_2]$ and $[\{Cp_2ErNHEt\}_2]$ is not surprising, since for the amido complex intermediate the charge flow from the OCN unit to the aromatic moiety, a prerequisite for further reactivity, is inhibited, only allowing the further nucleophilic reaction to take place at the nitrogen atom. The results represent a good example that the reactivity of ketenes toward organometallic complexes can be finely tuned simply by changing the nature of the amide ligands.

To determine the coordination geometry around the erbium ion in the new product, complex **7** was studied by X-ray analysis. Figure 5 confirms that complex **7** contains four PhEtCCO molecules that have been activated and inserted into two original Er–N bonds of $[\{Cp_2ErNHEt\}_2]$. The erbium ions are linked by double $[PhEtCHCON(Et)CO\text{-}CEtPh]^-$ anion bridges in an end-to-end coordinated fashion to form a dimetallic eight-coordinate complex; distances

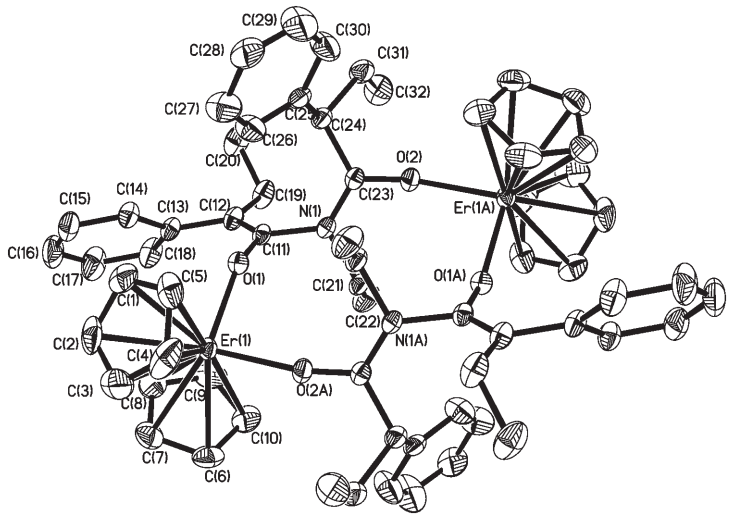

Figure 5. Molecular structure of complex **7** (thermal ellipsoids at 30% probability).

within and between the ligands are as expected. Table 5 shows selected bond lengths and angles for complex **7**. The

Table 5. Selected bond lengths [Å] and angles [°] of complex **7**.

Er(1)–O(1)	2.135(3)	Er(1)–C(5)	2.649(6)
Er(1)–O(2A)	2.234(3)	Er(1)–C(4)	2.653(7)
Er(1)–C(2)	2.621(6)	N(1)–C(23)	1.324(6)
Er(1)–C(8)	2.626(6)	N(1)–C(11)	1.462(5)
Er(1)–C(1)	2.626(6)	N(1)–C(21)	1.482(6)
Er(1)–C(10)	2.627(6)	O(1)–C(11)	1.311(5)
Er(1)–C(6)	2.627(6)	O(2)–C(23)	1.258(6)
Er(1)–C(9)	2.628(6)	O(2)–Er(1A)	2.234(3)
Er(1)–C(7)	2.631(6)	C(11)–C(12)	1.348(7)
Er(1)–C(3)	2.644(6)	C(23)–C(24)	1.524(7)
O(1)-Er(1)-O(2A)	93.25(13)	C(11)-O(1)-Er(1)	149.1(3)
C(23)-N(1)-C(11)	125.5(4)	C(23)-O(2)-Er(1A)	168.1(3)
C(23)-N(1)-C(21)	120.1(4)	O(2)-C(23)-N(1)	121.2(4)
C(11)-N(1)-C(21)	113.2(4)	O(2)-C(23)-C(24)	118.6(4)
C(23)-C(24)-C(31)	109.0(4)	N(1)-C(23)-C(24)	120.2(4)

C–O and C–N bond lengths suggest charge delocalization as shown in Scheme 5. The C(11)–O(1) and C(23)–O(2) distances of 1.311(5) and 1.258(6) Å, respectively, are between

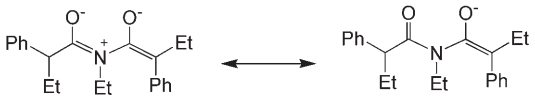

Scheme 5. Resonance structures of the anion obtained by double PhEtC-CO insertion into the Ln–N bond of [{Cp_2LnNHEt}$_2$].

the 1.293–1.407 Å range of C(sp^2)–O and the 1.192–1.256 Å range of C(sp^2)=O distances.[2b,41] The C(23)–N(1) bond length (1.324(6) Å) also lies between the typical C(sp^2)=N distance (1.279–1.329 Å) and the range of C(sp^2)–N distances (1.321–1.416 Å), while the C(11)–N(1) bond (1.462(5) Å) has a typical single-bond length.[2b] The Er(1)–O(1) (2.135(3) Å) and Er(1A)–O(2) (2.234(3) Å) bond lengths are within the range observed for Cp_2Er–OR bonds involving anionic oxygen donor ligands such as alkoxides[27] and are shorter than Cp_2ZEr–(OR_2) bonds (Z = a monoanionic ligand) for neutral oxygen donor ligands.[28]

Conclusion

Some unusual types of reactivities of rare-earth amide complexes toward ketenes have been established, and the results demonstrate that both electronic and steric factors play an important role in determining the chemo- and regioselectivities of ketene insertion into the Ln–N bond, and that organolanthanides can be expected to offer some distinctive reactivities beyond that possible with transition-metal complexes in the activation of ketenes. For example, we found that the lanthanocene moiety can induce an unprecedented regioselective conjugate electrophilic addition of ketene to the phenyl substituent of enolate ligands through negative charge delocalization, which represents a rare example of selective dearomatization of the pendent aryl group in organometallic chemistry and provides a new method for the functionalized dearomatization of aryl rings with a unique selectivity of the introduced substituents. The regioselective transformation of the pendent substituents of organolanthanides is particularly challenging, since the central metal strongly interacts with many of the reactants employed to result in the cleavage of the lanthanide–ligand bond as more facile reaction pathways;[45] further, no example of dearomatization of aromatic ketenes has also been reported previously. The above results demonstrate, for the first time, that the partial negative charge transfer from a coordinated heteroatom to the pendent aryl ring favors attack on the ring carbon atom by electrophiles. In addition, the observed lanthanocene moiety induced tandem dearomatization/rearomatization of the pendent phenyl ring also opens a new route to the acylation of arenas.

Furthermore, we observed that the reactivity of lanthanocene amide complexes toward ketenes is extremely susceptible to the nature of amide ligands, and the use of primary amide ligands can lead to the preferred isomerization of the newly formed amino-substituted enolate ligand to the amido ligand through a 1,3-hydrogen shift. The sterically demanding phenyl group offers a good stabilizing environment for the resulting lanthanide–amido species, while the less-bulky ethyl group allows the amido complex intermediate to react further with a second ketene molecule, forming another unusual double-insertion product without the direct linkage between two ketene molecules. The latter represents a novel pattern of ketene double insertion. Examples of double insertions without bond-formation between substrates are rare and are generally limited to the cycloaddition of organometallic complexes with dianionic ligands such as the imido ligand. In brief, the results presented here represent a good example that reactivity of ketenes toward organometallic complexes can be finely tuned simply by changing the nature of the amide ligands, metals, and ketenes. They provide a new insight into the ligand-forming and ligand-transforming behavior of organolanthanides and demonstrate the potential of the phenyl substituent in further functionalization. In addition, they also highlight distinctive reactivity of ketenes beyond that possible with other cumulenes, and exemplify their potential as functionalization reagents in synthetic chemistry.[46]

Experimental Section

General procedures: All operations involving air- and moisture-sensitive compounds were carried out under an inert atmosphere of purified nitrogen gas using standard Schlenk techniques. The solvents THF, toluene, and *n*-hexane were refluxed and distilled over sodium benzophenone ketyl under nitrogen gas prior to use. Elemental analyses for C, H, and N were carried out by using a Rapid CHN-O analyzer. Infrared spectra were obtained on a NICOLET FTIR 360 spectrometer with samples prepared as Nujol mulls. Mass spectra were recorded on a Philips HP5989 A instrument operating in the EI mode. Crystalline samples of the respective complexes were rapidly introduced by the direct inlet techniques with a source temperature of 300 K. The values of *m*/*z* refer to the isotopes ^{1}H, ^{12}C, ^{14}N, ^{16}O, ^{174}Yb, ^{166}Er, ^{89}Y, and ^{164}Dy. ^{1}H NMR data were obtained with a Bruker DMX-500 or Bruker Daltonics FTMS-7 NMR spectrometer. GC–MS data were obtained on a Finnigan Voyager instrument running in the EI mode.

The complexes [{Cp_2LnN*i*Pr$_2$}$_2$],[4f] [{Cp_2LnNHPh}$_2$],[37] diphenyl ketene,[47] and ethylphenyl ketene[48] were prepared according to the procedures described in the literature. *n*-Butyllithium, diisopropylamine, aniline, and ethylamine were purchased from commercial sources and were used without further purification.

Crystal structure determination for compounds 1b·1/4$C_6H_5CH_3$, 2a, 2b, 5a·2THF, 5b, 6, and 7·$C_6H_5CH_3$: Suitable single crystals of complexes **1b**·1/4$C_6H_5CH_3$, **2a**, **2b**, **5a**·2THF, **5b**, **6**, and **7**·$C_6H_5CH_3$ were sealed in thin-walled glass capillaries under nitrogen gas for the X-ray diffraction study. Diffraction data were collected on a Bruker SMART Apex CCD diffractometer by using graphite-monochromated $Mo_{K\alpha}$ (λ = 0.71073 Å) radiation. The intensities were corrected for Lorentz-polarization effects and empirical absorption with the SADABS program.[49] The structures were solved by the direct method by using the SHELXLS-97 program[50] and refined with all data by using the full-matrix least-squares method on F^2. The hydrogen atoms were included in calculated positions with iso-

tropic thermal parameters related to those of the supporting carbon atoms, but were not included in the refinement.

Crystallographic data for compounds **1b**·1/4 $C_6H_5CH_3$, **2a**, **2b**, **5a**·2 THF, **5b**, **6**, and **7**·$C_6H_5CH_3$ are shown in Tables 6 and 7. CCDC-260758 (**1b**), CCDC-260756 (**2a**), CCDC-260757 (**2b**), CCDC-260759 (**5a**), CCDC-295984 (**5b**), CCDC-295834 (**6**), and CCDC-295985 (**7**) contain the supplementary crystallographic data for this paper. These data can be obtained free of charge from the Cambridge Crystallographic Data Centre via www.ccdc.cam.ac.uk/data_request/cif.

Reaction of [{Cp_2YbN*i*Pr_2}$_2$] with diphenylketene: Diphenylketene (0.648 g, 3.34 mmol) was added to a solution of [{Cp_2YbN*i*Pr_2}$_2$] (0.674 g, 0.84 mmol) in toluene at −20 °C. After stirring at room temperature for 24 h, the solution was concentrated by reduced pressure to about 5 mL. Crystallization by vapor diffusion of hexane into the solution afforded compound **1a**·1/4 $C_6H_5CH_3$ as red crystals. Yield 0.816 g, 60 %; IR (Nujol): $\tilde{\nu}$ = 1591 (m), 1560 (s), 1491 (m), 1279 (s), 1138 (s), 1013 (s), 950 (m), 772 (m), 698 cm^{-1} (s); MS (EI): *m*/*z* (%): 792 (3) $[M]^+$, 692 (2) $[M-NiPr_2]^+$; elemental analysis calcd (%) for $C_{45.75}H_{46}O_2NYb$: C 67.60, H 5.70, N 1.55; found: C 67.49, H 5.69, N 1.68.

Reaction of [{Cp_2ErN*i*Pr_2}$_2$] with diphenylketene: Following the procedure described for complex **1a**, reaction of [{Cp_2ErN*i*Pr_2}$_2$] (0.603 g, 0.76 mmol) with Ph_2CCO (0.588 g, 3.04 mmol) gave **1b**·1/4 $C_6H_5CH_3$ as yellow crystals. Yield 0.882 g, 72 %; IR (Nujol): $\tilde{\nu}$ = 1646 (m), 1591 (m), 1565 (s), 1489 (m), 1281 (s), 1139 (s), 1012 (s), 956 (s), 770 (m), 698 cm^{-1} (s); MS (EI): *m*/*z* (%): 784 (5) $[M]^+$, 684 (2) $[M-NiPr_2]^+$; MS (ESI) of hydrolyzed product [$Ph_2CHCOC_6H_5$(=CPhCON*i*Pr_2)]: 490 $[M+H]^+$, 512 $[M+Na]^+$; elemental analysis calcd (%) for $C_{45.75}H_{46}O_2NEr$: C 67.91, H 5.73, N 1.73; found: C 67.82, H 5.64, N 1.70.

Reaction of [{Cp_2YbN*i*Pr_2}$_2$] with ethylphenylketene: Ethylphenyl ketene (0.464 g, 3.18 mmol) was added to a toluene solution of [{Cp_2YbN*i*Pr_2}$_2$] (0.643 g, 0.78 mmol, 40 mL) at −20 °C. After stirring at room temperature for 24 h, the solution was concentrated by reduced pressure to about 2 mL and crystallized at 0 °C to give complex **2a** as red crystals. Yield 0.83 g, 75 %; ^{1}H NMR (500 MHz, C_6D_6, 25 °C, TMS): δ = 8.04 (b, 2H; aryl ring), 7.10 (m, 7H; aryl ring), 3.78 (m, 1H; COC*H*C_2H_5), 3.47 (m, 2H; C*H*(CH_3)$_2$), 2.19 (s, 5H; C_5H_5), 2.34(m, 2H; C*H*$_2$$CH_3$), 1.97 (m, 2H; C*H*$_2$$CH_3$), 1.56–1.32 (m, 12H; CH(C*H*$_3$)$_2$), 0.83 (t, 6H; CH_2CH_3), 0.37 ppm (s, 5H; C_5H_5); IR (Nujol): $\tilde{\nu}$ = 1559 (s), 1014 (m), 776 (s), 697 cm^{-1} (m); MS (EI): *m*/*z* (%): 696 (2) $[M/2]^+$, 631 (9) $[M/2-Cp]^+$; elemental analysis calcd (%) for $C_{72}H_{88}O_4N_2Yb_2$: C 62.14, H 6.37, N 2.01; found: C 62.08, H 6.24, N 2.05.

Reaction of [{Cp_2ErN*i*Pr_2}$_2$] with ethylphenylketene: By using the procedure described for complex **2a**, the reaction of [{Cp_2ErN*i*Pr_2}$_2$] (0.418 g, 0.53 mmol) and PhEtCCO (0.307 g, 2.10 mmol) in toluene afforded complex **2b** as orange-yellow crystals. Yield 0.529 g, 73 %; IR (Nujol): $\tilde{\nu}$ = 1588 (s), 1557 (s), 1492 (s), 1325 (s), 1161 (s), 1141 (s), 1013 (s), 773 (s), 698 cm^{-1} (s); MS (EI): *m*/*z* (%): 688 (3) $[M/2]^+$; elemental analysis calcd (%) for $C_{72}H_{88}O_4N_2Er_2$: C 62.66, H 6.43, N 2.03; found: C 62.58, H 6.34, N 2.05.

Reaction of [{Cp_2DyN*i*Pr_2}$_2$] with ethylphenylketene: By using the procedure described for complex **2a**, the reaction of [{Cp_2DyN*i*Pr_2}$_2$] (0.420 g, 0.54 mmol) and PhEtCCO (0.312 g, 2.14 mmol) in toluene afforded complex **2c** as white powder. Yield 0.475 g, 65 %; IR (Nujol): $\tilde{\nu}$ = 1597 (s), 1557 (s), 1492 (s), 1304 (m), 1161 (s), 1091 (w), 1013 (s), 771 (s), 691 cm^{-1} (s); MS (EI): *m*/*z* (%): 686 (3) $[M/2]^+$; 621 (12) $[M/2-Cp]^+$; elemental analysis calcd (%) for $C_{72}H_{88}O_4N_2Dy_2$: C 63.25, H 6.35, N 1.99; found: C 63.17, H 6.43, N 2.05.

Reaction of [{Cp_2YbN*i*Pr_2}$_2$] with ethylphenylketene in THF: PhEtCCO (0.122 g, 0.836 mmol) was slowly dropped at −30 °C into a solution of [{Cp_2YbN*i*Pr_2}$_2$] (0.337 g, 0.418 mmol) in THF (30 mL). After stirring for 30 min at the low temperature, the mixture was warmed to room temperature and stirred for 48 h. The solution color slowly changed from dark green to red. Then, the solution was concentrated in vacuo to about 3 mL. Crystallization by diffusion of hexane into the solution in THF afforded compound **3** as orange-yellow powder. Yield 0.348 g, 67 %; IR (Nujol): $\tilde{\nu}$ = 1564 (s), 1493 (m), 1291 (m), 1081 (m), 1012 (s), 965 (w), 916 (w), 862 (w), 771 (s), 695 cm^{-1} (s); MS (EI): *m*/*z* (%): 550 (5) $[M-THF]^+$; GC–MS of the hydrolyzed product (PhEtCHCON*i*Pr_2): 247 $[M]^+$; ele-

Table 6. Crystal and data collection parameters of complexes **1b**·1/4 $C_6H_5CH_3$, **2a**, and **2b**.

	1b·1/4 $C_6H_5CH_3$	**2a**	**2b**
formula	$C_{45.75}H_{45}ErNO_2$	$C_{72}H_{68}N_2O_4Yb_2$	$C_{72}H_{88}Er_2N_2O_4$
molecular weight	808.09	1371.36	1379.96
crystal dimensions [mm]	0.25 × 0.25 × 0.30	0.30 × 0.20 × 0.20	0.35 × 0.25 × 0.15
crystal system	tetragonal	monoclinic	triclinic
space group	*P*4/*n*	*C*2/*c*	$P\bar{1}$
a [Å]	30.452(2)	28.076(5)	11.285(3)
b [Å]	30.452(2)	10.8737(18)	13.849(4)
c [Å]	8.7310(9)	25.955(4)	14.628(4)
α [°]	90	90	113.293(4)
β [°]	90	99.650(3)	106.546(4)
γ [°]	90	90	99.516(4)
V [Å^3]	8096.7(12)	7812(2)	1910.0(10)
Z	8	4	1
ρ_{calcd} [g cm^{-3}]	1.326	1.166	1.200
μ [mm^{-1}]	2.108	2.419	2.223
F (000)	3284	2744	702
T [K]	293(2)	293(2)	293(2)
scan type	$\omega-2\theta$	$\omega-2\theta$	$\omega-2\theta$
θ range [°]	1.34–25.01	1.59–25.01	1.98–25.01
no. reflections (measured)	32792	15972	8011
no. reflections (unique)	7151 (R_{int} = 0.0640)	6856 (R_{int} = 0.0518)	6619 (R_{int} = 0.0376)
completeness to θ	100.0 % (θ = 25.01)	99.6 % (θ = 25.01)	98.1 % (θ = 25.01)
max and min transmission	0.6207 and 0.5704	0.6433 and 0.5306	0.7316 and 0.5101
data/restraints/parameters	7151/0/452	6856/0/350	6619/0/347
goodness-of-fit on F^2	1.215	1.077	0.933
*R*1, *wR*2 [$I > 2\sigma(I)$]	0.0778, 0.1732	0.0672, 0.1612	0.0744, 0.1940
*R*1, *wR*2 (all data)	0.1131, 0.1869	0.1202, 0.1854	0.1339, 0.2259
largest diff peak and hole [e Å^{-3}]	+1.075/−2.021	+0.944/−0.567	+1.915/−0.857

Table 7. Crystal and data collection parameters for complexes **5a**·2THF, **5b**, **6** and **7**·$CH_3C_6H_5$.

	5a·2THF	**5b**	**6**	**7**·$CH_3C_6H_5$
formula	$C_{60}H_{68}N_2O_4Yb_2$	$C_{52}H_{52}N_2O_2Y_2$	$C_{60}H_{52}O_2N_2Er_2$	$C_{71}H_{80}Er_2N_2O_4$
molecular weight	1227.24	914.78	1167.56	1359.89
crystal dimensions [mm]	0.20×0.15×0.12	0.15×0.10×0.08	0.20×0.15×0.12	0.35×0.25×0.20
crystal system	triclinic	monoclinic	triclinic	triclinic
space group	$P\bar{1}$	$P2(1)/c$	$P\bar{1}$	$P\bar{1}$
a [Å]	8.601(3)	16.641(7)	9.818(3)	12.453(4)
b [Å]	12.021(4)	19.523(8)	10.586(3)	12.509(4)
c [Å]	13.684(4)	8.600(4)	12.998(4)	12.538(4)
α [°]	97.200(4)	90	68.033(4)	116.098(4)
β [°]	95.430(4)	99.674(6)	89.665(4)	109.198(4)
γ [°]	110.199(4)	90	75.940(5)	99.304(4)
V [Å^3]	1302.8(7)	2754(2)	1209.9(6)	1544.6(9)
Z	1	2	1	1
ρ_{calcd} [g cm^{-3}]	1.564	1.103	1.602	1.462
μ [mm^{-1}]	3.615	2.130	3.490	2.747
F (000)	614	944	578	688
T [K]	293(2)	293(2)	293(2)	293(2)
scan type	$\omega-2\theta$	$\omega-2\theta$	$\omega-2\theta$	$\omega-2\theta$
θ range [°]	1.52–25.00	1.62–25.01	1.70–25.01	1.86–25.01
no. reflections (measured)	5453	11176	5095	6460
no. reflections (unique)	4513 (R_{int}=0.0155)	4853 (R_{int}=0.1432)	4205 (R_{int}=0.0228)	5349 (R_{int}=0.0230)
completeness to θ	98.1% (θ=25.00)	99.9% (θ=25.01)	98.8% (θ=25.01)	98.3% (θ=25.01)
max and min transmission	0.6709 and 0.5317	0.8481 and 0.7406	0.6795 and 0.5420	0.6095 and 0.4464
data/restraints/parameters	4513/0/308	4853/0/244	4205/0/298	5349/5/358
goodness-of-fit on F^2	1.069	1.052	1.057	1.058
$R1$, $wR2$ [$I>2\sigma(I)$]	0.0286, 0.0713	0.1019, 0.2886	0.0373, 0.0888	0.0328, 0.0859
$R1$, $wR2$ (all data)	0.0323, 0.0742	0.2219, 0.3566	0.0450, 0.0935	0.0372, 0.0890
largest diff peak and hole [e Å^{-3}]	+1.862/−1.050	+1.136/−0.775	+1.625/−0.999	+1.562/−1.740

mental analysis calcd (%) for $C_{30}H_{42}O_2NYb$: C 57.96, H 6.81, N 2.25; found: C 57.90, H 6.70, N 2.15.

Synthesis of compound 4: Hydrolysis of **2a** or **2b** followed by extraction by using diethyl ether gave **4** as a light-yellow solid. ^{1}H NMR ($CDCl_3$, 500 MHz): δ=7.88 (d, 2H; C_6H_4), 6.98–7.29 (m, 7H; aryl ring), 4.41 (t, 1H; C*H*CO), 3.96 (m, 2H; C*H*Me$_2$), 3.52 (t, 1H; C*H*CON), 2.18 (m, 2H; CH_2CH$_3$), 1.87 (m, 2H; CH_2CH$_3$), 1.32 (m, 12H; CH(CH_3)$_2$), 0.89 (t, 3H; CH$_2$CH_3), 0.84 ppm (t, 3H; CH$_2$CH_3); MS (EI): m/z (%): 393 [M]$^+$.

Reaction of [{Cp$_2$YbNHPh}$_2$] with ethylphenylketene: PhEtCCO (0.307 g, 2.10 mmol) was added to a solution of [{Cp$_2$YbNHPh}$_2$] (0.415 g, 0.53 mmol) in toluene (30 mL) at −20 °C. After stirring at low temperature for 30 min, the mixture was warmed to ambient temperature and was stirred overnight. Then, the solvent was evaporated by reduced pressure. Recrystallization by vapor diffusion of hexane into a toluene/THF mixture afforded orange-yellow crystals of **5a**·2THF. Yield 0.483 g, 75%; IR (Nujol): $\tilde{\nu}$=1561 (s), 1492 (s), 1261 (s), 1182 (m), 1093 (s), 1018 (s), 801 (s), 770 cm^{-1} (s); MS (EI): m/z (%): 542 (40) [M/2]$^+$, 477 (42) [M/2−Cp]$^+$; elemental analysis calcd (%) for $C_{60}H_{68}O_4N_2Yb_2$: C 58.72, H 5.58, N 2.28; found: C 58.81, H 5.61, N 2.13.

Reaction of [{Cp$_2$YNHPh}$_2$] with ethylphenylketene: To a solution of [{Cp$_2$YNHPh}$_2$] (0.34 g, 0.54 mmol) in toluene (30 mL) was added PhEtCCO (0.157 g, 1.08 mmol) at −30 °C. After stirring for 30 min at this temperature, the mixture was slowly warmed to room temperature and was stirred overnight. Then the solution was concentrated and cooled at −18 °C to give complex **5b** as yellow crystals. Yield 0.341 g, 81%; IR (Nujol): $\tilde{\nu}$=1585 (s), 1496 (s), 1229 (s), 1170 (m), 1074 (s), 1012 (s), 970 (m), 771 cm^{-1} (s); MS (EI): m/z (%): 457 (30) [M/2]$^+$, 392 (33) [M/2−Cp]$^+$; ^{1}H NMR (C_6D_6, 500 MHz): δ=7.21–7.08 (m, 8H; C_6H_5), 6.45 (d, 2H; C_6H_5), 6.31 (s, 5H; C_5H_5), 6.23 (s, 5H; C_5H_5), 3.57 (t, 1H; C*H*Ph), 1.77 (m, 2H; CH_2CH$_3$), 0.78 ppm (t, 3H; CH$_2$CH_3); elemental analysis calcd (%) for $C_{52}H_{52}O_2N_2Y_2$: C 68.28, H 5.73, N 3.06; found: C 68.14, H 5.78, N 3.09.

Reaction of [{Cp$_2$ErNHPh}$_2$] with diphenylketene: By using the procedure described for **5a**, reaction of [{Cp$_2$ErNHPh}$_2$] (0.437 g, 0.56 mmol) with Ph$_2$CCO (0.217 g, 1.12 mmol) gave **6** as pink crystals. Yield 0.543 g, 83%; IR (Nujol): $\tilde{\nu}$=1586 (s), 1491 (s), 1217 (s), 1009 (s), 970 (s), 770 cm^{-1} (s); MS (EI): m/z (%): 582 (5) [M/2]$^+$, 517 (2) [M/2−Cp]$^+$; elemental analysis calcd for $C_{60}H_{52}O_2N_2Er_2$: C 61.72, H 4.49, N 2.40; found: C 61.89, H 4.41, N 2.34.

Reaction of [{Cp$_2$ErNHEt}$_2$] with ethylphenylketene: By using the procedure described for **5a**, the reaction of [{Cp$_2$ErNHEt}$_2$] (0.34 mg, 0.50 mmol) and PhEtCCO (0.291 g, 1.99 mmol) in toluene afforded compound **7**·$C_6H_5CH_3$ as pink crystals. Yield 0.381 g, 56%; IR (Nujol): $\tilde{\nu}$= 3093 (m), 2729(m), 1959 (m), 1751 (m), 1627 (s), 1564 (s), 1460 (s), 1213 (s), 1176 (s), 1011 (m), 947 (s), 908 (s), 815 (s), 771 (s), 630 cm^{-1} (s); elemental analysis calcd (%) for $C_{71}H_{80}Er_2N_2O_4$: C 62.71, H 5.93, N 2.06; found: C 62.58, H 6.00, N 2.09.

Acknowledgements

We thank the NNSF of China, NSF of Shanghai, the Fund of the New Century Distinguished Scientist of the Education Ministry of China, and the Research Fund for the Doctoral Program of Higher Education of China for financial support.

[1] a) W. J. Evans, B. L. Davis, *Chem. Rev.* **2002**, *102*, 2119–2136; b) G. M. Ferrence, J. Takats, *J. Organomet. Chem.* **2002**, *647*, 84–93; c) X. G. Zhou, M. Zhu, *J. Organomet. Chem.* **2002**, *647*, 28–49.

[2] a) O. Tardif, D. Hashizume, Z. M. Hou, *J. Am. Chem. Soc.* **2004**, *126*, 8080–8081; b) W. J. Evans, C. H. Fujimoto, J. W. Ziller, *Organometallics* **2001**, *20*, 4529–4536; c) W. J. Evans, J. M. Perotti, S. A. Kozimor, T. M. Champagne, B. L. Davis, G. W. Nyce, C. H. Fujimoto, R. D. Clark, M. A. Johnston, J. W. Ziller, *Organometallics* **2005**, *24*, 3916–3931; d) W. J. Evans, K. A. Miller, J. W. Ziller, *Inorg. Chem.* **2006**, *45*, 424–429.

[3] H. R. Li, Y. M. Yao, Q. Shen, L. H. Weng, *Organometallics* **2002**, *21*, 2529–2532.

[4] a) J. Zhang, L. P. Ma, R. F. Cai, L. H. Weng, X. G. Zhou, *Organometallics* **2005**, *24*, 738–742; b) J. Zhang, R. F. Cai, L. H. Weng, X. G. Zhou, *Organometallics* **2003**, *22*, 5385–5391; c) X. G. Zhou, L. B. Zhang, M. Zhu, R. F. Cai, L. H. Weng, Z. X. Huang, Q. J. Wu, *Organometallics* **2001**, *20*, 5700–5706; d) Q. Shen, H. R. Li, C. S. Yao, Y. M. Yao, L. L. Zhang, K. B. Yu, *Organometallics* **2001**, *20*, 3070–3073; e) W. J. Evans, K. J. Forrestal, J. W. Ziller, *J. Am. Chem. Soc.* **1998**, *120*, 9273–9282; f) L. Mao, Q. Shen, M. Q. Xue, J. Sun, *Organometallics* **1997**, *16*, 3711–3714.

[5] a) L. P. Ma, J. Zhang, R. F. Cai, Z. X. Chen, L. H. Weng, X. G. Zhou, *J. Organomet. Chem.* **2005**, *690*, 4926–4932; b) J. Zhang, R. F. Cai, L. H. Weng, X. G. Zhou, *Organometallics* **2004**, *23*, 3303–3308; c) J. Zhang, R. F. Cai, L. H. Weng, X. G. Zhou, *J. Organomet. Chem.* **2003**, *672*, 94–99; d) J. Zhang, R. Y. Ruan, Z. H. Shao, R. F. Cai, L. H. Weng, X. G. Zhou, *Organometallics* **2002**, *21*, 1420–1424; e) G. R. Giesbrecht, G. D. Whitener, J. Arnold, *J. Chem. Soc. Dalton Trans.* **2001**, 923–927.

[6] a) S. Tobisch, *Chem. Eur. J.* **2005**, *11*, 6372–6385; b) S. Tobisch, *J. Am. Chem. Soc.* **2005**, *127*, 11979–11988; c) S. Tobisch, *Chem. Eur. J.* **2005**, *11*, 3113–3126; d) K. Komeyama, D. Sasayama, T. Kawabata, K. Takeira, K. Takaki, *Chem. Commun.* **2005**, 634–636.

[7] S. Hong, T. J. Marks, *Acc. Chem. Res.* **2004**, *37*, 673–686.

[8] G. L. Geoffroy, S. L. Bassner, *Adv. Organomet. Chem.* **1988**, *28*, 1–83.

[9] a) E. Hevia, J. Pérez, V. Riera, D. Miguel, *Organometallics* **2003**, *22*, 257–263; b) D. D. Vanderlende, K. A. Abboud, J. M. Boncella, *Inorg. Chem.* **1995**, *34*, 5319–5326.

[10] E. Hevia, J. Pérez, V. Riera, D. Miguel, P. Campomanes, M. I. Menéndez, T. L. Sordo, S. García-Granda, *J. Am. Chem. Soc.* **2003**, *125*, 3706–3707.

[11] C. M. Zhang, R. T. Liu, X. G. Zhou, Z. X. Chen, L. H. Weng, Y. H. Lin, *Organometallics* **2004**, *23*, 3246–3251.

[12] a) H. Schumann, J. A. Meese-Marktscheffel, L. Esser, *Chem. Rev.* **1995**, *95*, 865–986; b) F. T. Edelmann, D. M. M. Freckmann, H. Schumann, *Chem. Rev.* **2002**, *102*, 1851–1896; c) S. Arndt, J. Okuda, *Chem. Rev.* **2002**, *102*, 1953–1976; d) N. Marques, A. Sella, J. Takats, *Chem. Rev.* **2002**, *102*, 2137–2160; e) F. Nief, *Coord. Chem. Rev.* **1998**, *180*, 13–81; f) *Fundamental and Technological Aspects of Organo-f-Element Chemistry* (Eds.: T. J. Marks, I. L. Fragala), Reidel, Dordrecht, **1985**, pp. 414.

[13] a) T. Bach, *Angew. Chem*, **1996**, *108*, 795–796; *Angew. Chem. Int. Ed. Engl.* **1996**, *35*, 729–730; b) A. R. Pape, K. P. Kaliappan, E. P. Kündig, *Chem. Rev.* **2000**, *100*, 2917–2940; c) W. D. Harman, *Chem. Rev.* **1997**, *97*, 1953–1978; d) W. D. Harman, *Coord. Chem. Rev.* **2004**, *248*, 853–866; e) B. C. Brooks, T. B. Gunnoe, W. D. Harman, *Coord. Chem. Rev.* **2000**, *206*, 3–61; f) J. M. Keane, W. D. Harman, *Organometallics* **2005**, *24*, 1786–1798; g) E. P. Kündig, *Transition Metal Arene π Complexes in Organic Synthesis and Catalysis*, Springer, Berlin, **2004**.

[14] a) J. Cornelisse, *Chem. Rev.* **1993**, *93*, 615–669; b) P. W. Rabideau, Z. Marcinow, *Org. React.* **1992**, *42*, 1–334; c) A. G. Schultz, *Acc. Chem. Res.* **1990**, *23*, 207–213; d) K. Nishiwaki, T. Ogawa, K. Matsuo, *Angew. Chem.* **2002**, *114*, 502–504; *Angew. Chem. Int. Ed.* **2002**, *41*, 484–486.

[15] a) A. G. Schultz, *Chem. Commun.* **1999**, 1263–1271; b) K. C. Nicolaou, D. Vourloumis, N. Winssinger, P. S. Baran, *Angew. Chem.* **2000**, *112*, 46–126; *Angew. Chem. Int. Ed.* **2000**, *39*, 44–122; c) J. L. Zhu, N. P. Grigoriadis, J. P. Lee, J. A. Porco, *J. Am. Chem. Soc.* **2005**, *127*, 9342–9343.

[16] a) G. Bernardinelli, S. Gillet, P. Kundig, R. G. Liu, A. Ripa, L. Saudan, *Synthesis* **2001**, *13*, 2040–2054; b) E. P. Kundig, D. P. Simmons, *J. Chem. Soc. Chem. Commun.* **1983**, *22*, 1320–1322.

[17] a) K. Maruoka, M. Ito, H. Yamamoto, *J. Am. Chem. Soc.* **1995**, *117*, 9091–9092; b) J. Barluenga, A. A. Trabanco, J. Flórez, S. Garcia-Granda, E. Martín, *J. Am. Chem. Soc.* **1996**, *118*, 13099–13100.

[18] a) X. G. Zhou, Z. E. Huang, R. F. Cai, L. B. Zhang, L. X. Zhang, X. Y. Huang, *Organometallics* **1999**, *18*, 4128–4133; b) X. G. Zhou, H. Z. Ma, X. Y. Huang, X. Z. You, *J. Chem. Soc. Chem. Commun.* **1995**, 2483–2484.

[19] a) H. Yasuda, H. Yamamoto, K. Yokota, S. Miyake, A. Nakamura, *J. Am. Chem. Soc.* **1992**, *114*, 4908–4910; b) M. A. Giardello, Y. Yamamoto, L. Brard, T. J. Marks, *J. Am. Chem. Soc.* **1995**, *117*, 3276–3277; c) Z. M. Hou, T. Yoshimura, Y. Wakatsuki, *J. Am. Chem. Soc.* **1994**, *116*, 11169–11170; d) T. Yoshimura, Z. M. Hou, Y. Wakatsuki, *Organometallics* **1995**, *14*, 5382–5392.

[20] M. Bao, H. Nakamura, Y. Yamamoto, *J. Am. Chem. Soc.* **2001**, *123*, 759–760.

[21] a) H. Yamazaki, P. B. Hong, *J. Mol. Catal.* **1983**, *21*, 133–150; b) T. Hattori, N. Koike, T. Satoh, S. Miyano, *Tetrahedron Lett.* **1995**, *36*, 4821–4824; c) G. Bartoli, *Acc. Chem. Res.* **1984**, *17*, 109–115.

[22] W. J. Evans, L. A. Hughes, D. K. Drummond, H. Zhang, J. L. Atwood, *J. Am. Chem. Soc.* **1986**, *108*, 1722–1723.

[23] I. L. Fedushkin, M. N. Bochkarev, G. A. Razuvaev, H. Schumann, *Chem. Eur. J.* **2001**, *7*, 3558–3563.

[24] W. J. Evans, J. W. Grate, R. J. Doedens, *J. Am. Chem. Soc.* **1985**, *107*, 1671–1679.

[25] W. J. Evans, R. Dominguez, T. P. Hanusa, *Organometallics* **1986**, *5*, 1291–1296.

[26] M. D. Curtis, S. Thanedar, W. M. Butler, *Organometallics* **1984**, *3*, 1855–1859.

[27] Y. J. Luo, Y. M. Yao, Q. Shen, Y. Xing, *J. Rare Earths* **2002**, *20*, 374–377.

[28] a) G. R. Willey, T. J. Woodman, W. Errington, *J. Indian Chem. Soc.* **1998**, *75*, 435–438; b) M. S. Cheung, H. S. Chan, Z. W. Xie, *Organometallics* **2005**, *24*, 4468–4474.

[29] a) P. Braunstein, D. Nobel, *Chem. Rev.* **1989**, *89*, 1927–1945; b) H. P. Wang, H. W. Li, Z. W. Xie, *Organometallics* **2003**, *22*, 4522–4531.

[30] M. Nishiura, Z. M. Hou, *J. Mol. Catal. A* **2004**, *213*, 101–106.

[31] a) R. Duchateau, T. Tuinstra, E. A. C. Brussee, A. Meetsma, P. Th. van Duijnen, J. H. Teuben, *Organometallics* **1997**, *16*, 3511–3522; b) R. Duchateau, C. T. van Wee, J. H. Teuben, *Organometallics* **1996**, *15*, 2291–2302.

[32] a) W. J. Evans, A. L. Wayda, W. E. Hunter, J. L. Atwood, *J. Chem. Soc. Chem. Commun.* **1981**, *14*, 706–708; b) W. J. Evans, K. J. Forrestal, J. W. Ziller, *J. Am. Chem. Soc.* **1995**, *117*, 12635–12636.

[33] a) Y. R. Wang, Q. Shen, L. P. Wu, Y. Zhang, J. Sun, *J. Organomet. Chem.* **2001**, *626*, 176–180; b) Z. W. Ye, Y. F. Yu, S. W. Wang, X. G. Jin, *J. Organomet. Chem.* **1993**, *448*, 91–93; c) G. Massarweh, R. D. Fischer, *J. Organomet. Chem.* **1993**, *444*, 67–74.

[34] a) G. A. Olah, *Friedel-Crafts and Related Reactions*, *Vol. I-IV*, Wiley-Interscience, New York, **1964**; b) S. Akai, A. J. Peat, S. L. Buchwald, *J. Am. Chem. Soc.* **1998**, *120*, 9119–9125.

[35] J. Frey, Z. Rappoport, *J. Am. Chem. Soc.* **1996**, *118*, 3994–3995.

[36] U. Segerer, J. Sieler, E. Hey-Hawkins, *Organometallics* **2000**, *19*, 2445–2449.

[37] J. E. Bercaw, D. L. Davies, P. T. Wolczanski, *Organometallics* **1986**, *5*, 443–450.

[38] a) C. T. Qian, B. Wang, D. L. Deng, J. Hu, *Inorg. Chem.* **1994**, *33*, 3382–3388; b) X. G. Zhou, Z. Z. Wu, Z. S. Jin, *J. Organomet. Chem.* **1992**, *431*, 289–296.

[39] Z. Z. Wu, Z. Xu, X. Z. You, *Polyhedron* **1992**, *11*, 2673–2678.

[40] X. G. Zhou, W. W. Ma, Z. E. Huang, *J. Organomet. Chem.* **1997**, *546*, 309–314.

[41] F. H. Allen, O. Kennard, D. G. Watson, L. Brammer, A. G. Orpen, *J. Chem. Soc. Perkin Trans.* **1987**, S1–S19.

[42] a) J. Holton, M. F. Lappert, D. G. H. Ballard, R. Pearce, J. L. Atwood, W. E. Hunter, *J. Chem. Soc. Dalton Trans.* **1979**, 54–61; b) J. Holton, M. F. Lappert, D. G. H. Ballad, R. Pearce, J. L. Atwood, W. E. Hunter, *J. Chem. Soc. Chem. Commun.* **1976**, 425–426.

[43] D. R. van Staveren, J. G. Haasnoot, A. M. Manotti-Lanfredi, S. Menzer, P. J. Nieuwenhuizen, A. L. Spek, F. Ugozzoli, J. Reedijk, *Inorg. Chim. Acta* **2000**, *307*, 81–87.

[44] A. J. Blake, P. Mountford, G. I. Nikonov, D. Swallow, *Chem. Commun.* **1996**, 1835–1836.

[45] a) H. Schumann, A. Heim, J. Demtschuk, S. H. Mühle, *Organometallics* **2003**, *22*, 118–128; b) W. J. Evans, J. M. Perotti, J. C. Brady, J. W. Ziller, *J. Am. Chem. Soc.* **2003**, *125*, 5204–5212; c)X. G. Zhou,

M. Zhu, L. B. Zhang, Z. Y. Zhu, C. F. Pi, Z. Pang, L. H. Weng, R. F. Cai, *Chem. Commun.* **2005**, 2342–2344.

[46] a) T. T. Tidwell, *Angew. Chem.* **2005**, *117*, 5926–5933; *Angew. Chem. Int. Ed.* **2005**, *44*, 5778–5785; b) T. T. Tidwell, *Angew. Chem.* **2005**, *117*, 6973–6975; *Angew. Chem. Int. Ed.* **2005**, *44*, 6812–6814; c) S. L. Wiskur, G. C. Fu, *J. Am. Chem. Soc.* **2005**, *127*, 6176–6177.

[47] E. D. Tailor, A. McKillop, G. H. Hawks, *Org. Synth.* **1972**, *52*, 36–48.

[48] L. M. Baigrie, H. R. Seiklay, T. T. Tidwell, *J. Am. Chem. Soc.* **1985**, *107*, 5391–5396.

[49] G. M. Sheldrick, SADABS, A Program for Empirical Absorption Correction, Göttingen (Germany), **1998**.

[50] G. M. Sheldrick, SHELXL-97, Program for the Refinement of the Crystal Structure, University of Göttingen, Göttingen (Germany), **1997**.

Received: February 5, 2006
Published online: June 6, 2006

